Formation of Cubic GaN Nanocrystals: A Study of the Thermal Stability of GaP Nanocrystals under Nitrogen

Shanmin Gao,[a] Liying Zhu,[a] Yi Xie,*[a] and Xiaobo Qian[a]

Keywords: Gallium / Phosphorus / Nitrides / Nanostructures / Thermochemistry

Cubic GaN nanoparticles and nanorods have been successfully synthesized from the nitridation of nanocrystalline GaP at 500 °C for 30 min, by manipulating different heating rates in nitrogen. The results of the thermal stability studies of nanocrystalline GaP under N_2 at different heating rates support the idea that cubic GaN can form from GaP via a N–P metathesis mechanism. The morphology of the cubic GaN can be controlled by variation of the external synthetic parameters such as the rate of heating. This work shows that it is very simple to synthesize cubic GaN nanoparticles or nanorods and opens a wide route towards detailed studies of the fundamental properties and potential applications of semiconductor nanocrystals.

Introduction

Nanostructures have potential for unique applications in electronics, optoelectronics and catalysis due to their high surface-to-volume ratios, quantum confinement effects and high fraction of chemically similar surface sites.[1,2] Wide band-gap semiconductor compound nanomaterials of the 13−15 group, such as GaN, GaP and GaAs are important in fundamental physics and are widely used for high-speed digital circuits, electronic and optoelectronic devices.[3] Over the past several years, considerable efforts have been made to explore new and simple synthetic routes to group 13−15 semiconductor nanocrystals.[4−7]

Of this group of semiconductors, the properties of GaN nanocrystals have received the least attention due to the difficulty involved in their preparation. Of the limited studies on GaN nanocrystals which have been reported, most have focused on hexagonal GaN with the wurtzite structure.[8−12] In comparison, cubic GaN nanocrystals have generally been studied in the form of thin films.[13−15] A recent report of cubic GaN powder synthesis via ammonolysis under thermal conditions required over 2700 atm of NH_3 pressure for over 24 h and the resultant product was generally found to be mixed with hexagonal phase GaN.[16] Moreover, cubic GaN has advantageous physical properties compared with those of the hexagonal phase, such as easier *p*-type doping, easier cleaving for laser facets, and a narrower energy band gap which means it is easier to reach the blue and green region.[17] Studies of the synthesis of cubic GaN nanocrystals is therefore of great importance.

Low-dimensional crystal structures, geometries such as wires, rods, and thin films are currently the focus of much attention due to their special properties.[18−20] These fascinating systems are expected to exhibit remarkable mechanical, electrical, optical and magnetic properties. Such low-dimensional crystalline materials have potential applications in molecular based electronic devices such as optical memory and in switches, displays and data records. Several approaches have been successfully developed for the fabrication of such nanowires and nanorods and their morphologies, microstructures and growth mechanisms have been studied.[21−25]

The synthesis, optical properties and catalytic reactivity of GaP nanocrystals have been studied in detail by our group.[26−28] The growth process and stability of GaP nanocrystals under thermal conditions in benzene have also been studied and a method for controlling the reaction process and uniformity of GaP grains has been reported.[29]

As is already known, the application of semiconductors depends on the change in the environmental conditions, so studying the influence of such conditions on the properties of semiconductor nanomaterials is also important. In this study, the thermal stability of GaP nanocrystals under a nitrogen atmosphere was investigated in detail and resulted in the establishment of a new preparative route to cubic GaN nanoparticles and nanorods.

Results and Discussion

XRD patterns were used to examine the crystal structures and phase purities of the products which were obtained by heating GaP nanoparticles at 500 °C for 30 min.

[a] Structure Research Laboratory and
Department of Chemistry,
University of Science and Technology of China,
Hefei, Anhui 230026, P. R. China
Fax: (internat.) +86-551-3603987
E-mail: yxielab@ustc.edu.cn

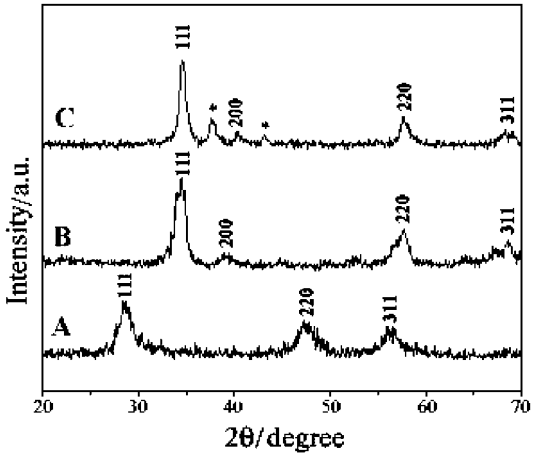

Figure 1. XRD patterns of (A) the starting GaP nanocrystals (B) the pure cubic GaN sample prepared from the heat treatment of GaP nanocrystals at 500 °C for 30 min with a heating rate of 5 °C/min and 10 °C/min (C) the cubic GaN sample prepared from the heat treatment of GaP nanocrystals at 500 °C for 30 min with a heating rate of 20 °C/min, the note * labels the residual elemental Ga

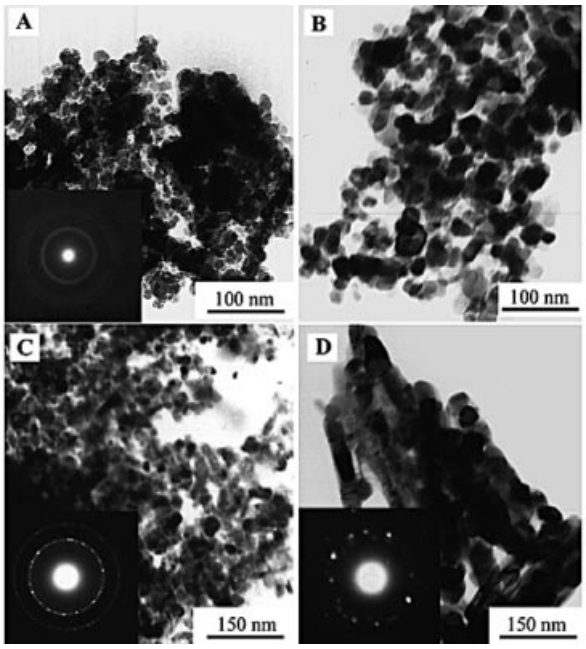

Figure 2. (A) TEM image of the starting GaP nanocrystals (B), (C) and (D) TEM images of cubic GaN obtained from heat treatment of GaP nanocrystals in N_2 at 500 °C for 30 min at heating rates of 5 °C/min, 10 °C/min and 20 °C/min, respectively; the picture insets are the SAED patterns of the corresponding materials

Figure 1 (A) displays the XRD pattern of the starting GaP nanocrystals. Pure cubic GaN was obtained from GaP nanocrystals at a low heating rate (≤10 °C/min) under N_2 at 500 °C for 30 min and the corresponding XRD pattern is shown in Figure 1 (B). All the reflections at $2\theta = 35.5$, 40.5, 58 and 68.5°, were indexed to the (111), (200), (220) and (311) lattice planes of cubic GaN, respectively. The calculated lattice parameter of cubic GaN using a computer simulation is $a_0 = 4.502 \pm 0.004$ Å, which is good agreement with the reported value.[17]

Figure 1 (C) shows the XRD pattern of the product prepared from the heat treatment of GaP nanocrystals under N_2 at 500 °C for 30 min at a heating rate of 20 °C/min, indicating that the product is cubic GaN coexisting with a minor amount elemental Ga (denoted as *, JC,PDF File, No. 31-0539). The minor elemental Ga can be easily removed by treatment using 1 N hydrochloric acid and pure cubic GaN can be obtained and its identity confirmed by its XRD pattern which is similar to that in Figure 1 (B). The XRD patterns of all the products are quite different from that of the starting GaP nanoparticles. The above results show that cubic GaN is formed by the heat treatment GaP nanocrystals under N_2 via a P−N metathesis reaction.

The morphology and structure of the prepared cubic GaN nanocrystallites were further characterized using transmission electron microscopy (TEM). Figure 2 (A) shows that the starting GaP nanocrystals are uniform spherical particles with a diameter of 8 ± 2 nm. Figure 2 (B and C) show that the cubic GaN obtained under N_2 at 500 °C for 30 min are uniform spherical particles with a diameter of 16 ± 2 nm for the product obtained with a heating rate of 5 °C/min and 22 ± 3 nm for the product obtained with a heating rate of 10 °C/min, in good agreement with the XRD result in which the average size can be calculated by employing the Scherrer equation. They exhibit the same morphology as the starting GaP nanocrystallites, the only difference being that the resultant GaN nanocrystals are larger than the starting GaP nanocrystallites due to the heat treatment at 500 °C. The SAED pattern [inset of Figure 2 (C)] shows diffraction rings consistent with the (111), (200), and (220) lattice plane of the cubic GaN phase. Except for the cubic GaN obtained at 500 °C for 30 min with a heating rate of 20 °C/min, the morphologies of the products [Figure 2 (D)] are different from the product obtained at 500 °C for 30 min with a heating rate of 10 °C/min in which nanorods are formed with diameters of 25 −30 nm and lengths of 200 −500 nm.

X-ray photoelectron spectroscopy (XPS) was used to investigate the elemental composition of the starting GaP nanocrystals and the above prepared GaN nanocrystals. The XPS results can provide evidence for the formation of GaN. Higher resolution spectra were taken of the Ga_{3d} and N_{1s} regions. The XPS spectra are shown in Figure 3. The binding energy values of the Ga_{3d} and N_{1s} core levels agree well with their chemical environments in cubic GaN. This clearly indicates that the N_2 molecules must be chemically bonded to Ga atoms, presumably forming N−Ga bonds.

The above results indicate that the P−N metathesis reaction occurred regardless of the heating rates used in our experiments . The replacement of P by N atoms is facilitated by the fact that P is more volatile than Ga and tends to escape from GaP upon thermal annealing. Traditionally, nitridation reactions using N_2 need high temperature (>1000 °C), since N_2 is very inert and stable. Small GaN crystals have been synthesized from molten gallium and N_2 at 700 °C in an alkali metal flux[30,31] and nanorod architectures have been prepared from catalyzed reactions between

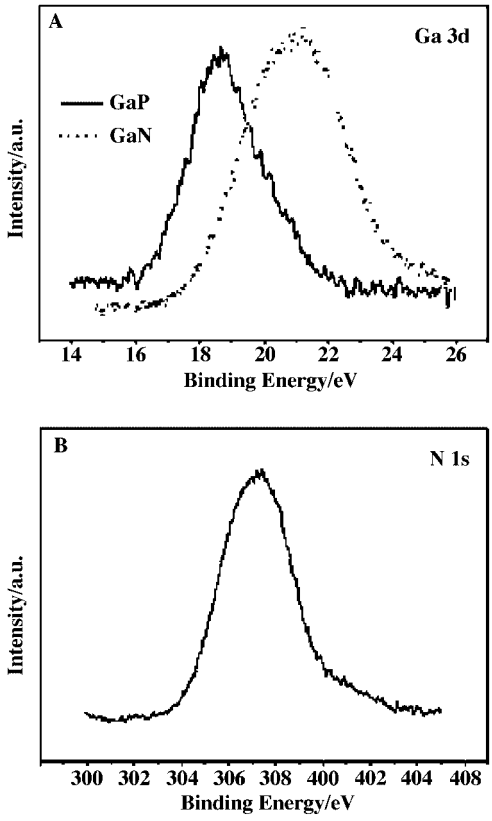

Figure 3. XPS spectra of the Ga_{3d} (A) and N_{1s} (B) core levels; the solid line represents the raw material GaP nanocrystals and the broken line represents the prepared cubic GaN obtained by heat treatment of GaP nanocrystals in N_2 at 500 °C for 30 min with a heating rate of 10 °C/min

gallium and NH_3 above 900 °C.[32,33] Our experiments indicate that cubic GaN can form at lower temperatures and shorter reaction times, an observation which is based on the high surface-to-volume ratio of nanocrystalline raw materials of GaP which can remarkably reduce the difficulty of nitridation. The GaP particles sizes significantly affect the nitridation reaction. The nitridation process may become more difficult or even incomplete and when the particle sizes reach the micron dimension, XRD results indicate that no GaN forms at all. Furthemore, at different heating rates the synthesized GaN exhibits different nanoscale morphologies, which leads us to believe that different heating rates cause different reaction mechanisms. The mechanisms of the surface adsorption reaction on GaP nanocrystals, and the formation of cubic GaN nanoparticles and nanorods are shown schematically in Scheme 1.

Regardless of the heating rates used in our experiments, the initial process involves the desorption of P atoms from the starting GaP nanocrystallites, adsorption of N atoms on the GaP surface and the further nitridation reaction [Scheme 1 (A)]. As is known, the surface area of nanocrystals is much larger than the bulk materials and there exist many vacancies and dangling bonds on the surface. In our experiments, the N_2 molecules are adsorbed onto the surface of the starting GaP nanocrystals during the initial stage of heating [Scheme 1 (A1)]. Firstly N_2 is adsorbed on

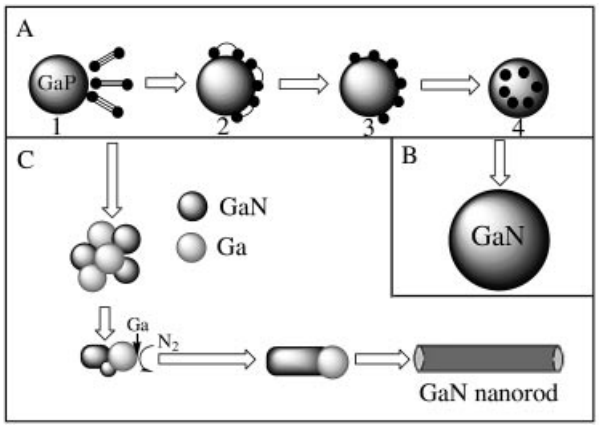

Scheme 1. The proposed mechanism for the formation of cubic GaN nanocrystals; (A) the surface adsorption reaction of N_2 on GaP nanocrystals and the nucleation of GaN; (B) the growth of GaN nanoparticles at lower heating rates; (C) step growth of GaN nanorods at higher heating rates

to the surface of the GaP nanocrystals (adsorbent), the physical adsorption depending on the van der Waals force. The vacancies and dangling bonds on the surface of the GaP nanocrystals provide a favorable environment for N_2 molecules to form bonds. Upon elevating the temperature, chemical bonding of N and Ga results, producing the activated adsorption. As a result, the N_2 molecules can be activated on the surface of GaP nanocrystals at a rather low temperature, remarkably weakening the strength of the N≡N bond on the surface of the GaP nanocrystals [Scheme 1 (A2)]. After the activated N atoms have formed [Scheme 1 (A3)] the N−P metathesis reaction can take place [Scheme 1 (A4)]. Since the metathesis reaction involves conversion of one zinc blende structure to another zinc blende structure this reaction can therefore be called a topotactic transformation.

At a lower heating rate (≤10 °C/min), the desorption of P, absorption of N and nitridation of GaP is a synchronous process on the GaP nanocrystals with no formation of excess Ga droplets, an observation which has been validated by the XRD pattern [as shown in Figure 1 (B)]. Thus GaN gradually forms on the surface of the GaP nanoparticles during this process. The total reaction can be described as in Equation (1).

$$GaP + N_2 \rightarrow GaN + P \quad (1)$$

The high surface area and reactivity of nanocrystalline GaP directly result in the formation of cubic GaN at lower temperature, lower pressure and shorter reaction times [Scheme 1 (B)]. The resultant GaN nanoparticles inherit the GaP matrixes in terms of structure and morphology which explains the similarity between the structures and morphologies of the resultant GaN and the starting GaP.

When the heating rate is higher (≥20 °C/min), however, the reaction is complicated and the initial chemical reaction is the desorption of P from the GaP nanocrystals, as described in Equation (2).

$$GaP \rightarrow Ga + P \quad (2)$$

The desorption chemical reaction is dominant and rapid and so the newly formed gallium has high activity and can react with N_2 to produce GaN nuclei, Equation (3).

$$Ga + N_2 \rightarrow GaN \quad (3)$$

A higher heating rate also promotes gallium coalescence along with its nitridation resulting in the appearance of smaller droplets of Ga. GaN nuclei start to aggregate and act as the nucleation seeds, then, stepwise growth proceeds with Ga droplets being pushed outward by the descending GaN [Scheme 1 (C)]. The Ga droplets play a crucial role in the growth of GaN nanorods based on the vapor-solid (VS) mechanism which is widely used to explain the growth of fiber-like semiconductors.[34] VS growth is apparently supported by the large Ga surface area and high reactivity which increases the effective steady-state Ga vapor pressure. The system is not in equilibrium because the Ga vapor reacts to form GaN. The increased rate of evaporation afforded by the large surface area of Ga more than likely produces a larger *steady-state* vapor pressure than is present over larger and coarser Ga particles. Scheme 1 (C) schematically depicts the mechanism of the formation of cubic GaN nanorods. More evidence has been provided by the supplementary experiments undertaken with a heating rate of 50 °C/min. The crystal structures and phase purities of the products are shown in Figure 4 (A) and the morphologies of the nanocrystalline GaN samples are shown in Figure 4 (B). The XRD pattern of the product prepared from the heat treatment of GaP nanocrystals under N_2 at 500 °C for 30 min with a heating rate of 50 °C/min indicates that the product is cubic GaN coexisting with a minor amount of elemental Ga (denoted as *) supporting that idea that cubic GaN nanorods can be obtained at the higher heating rate and the growth of GaN nanorods is based on the vapor-solid (VS) mechanism.

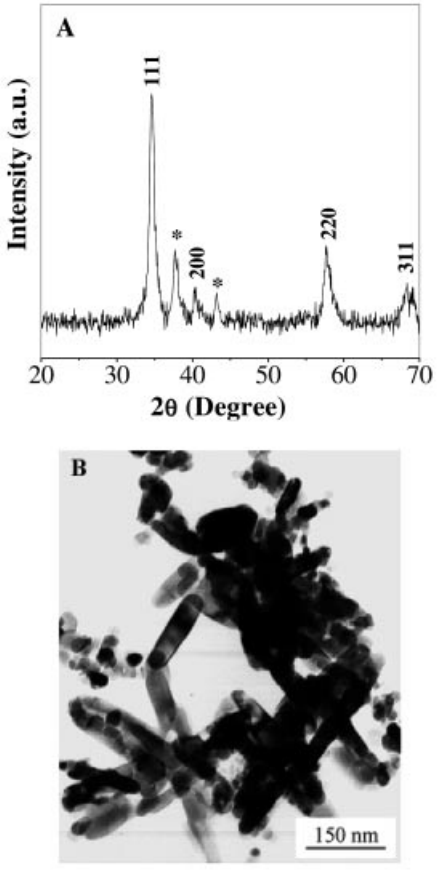

Figure 4. XRD pattern (A) and TEM image (B) of cubic GaN obtained from heat treatment of GaP nanocrystals at 500 °C for 30 min in N_2 with a heating rate of 50 °C/min

The above mechanism showing that cubic GaN can form in GaP via P−N metathesis is directly supported by the thermal stability study of GaP nanocrystals under nitrogen. At a lower heating rate, the desorption of P and nitridation are synchronous processes and, accordingly, the weight loss should be slow. At a higher heating rate, however, the desorption of P is preferential, so the weight loss should be rapid. In order to validate this, the thermogravimetric analysis (TGA) technique was used to analyze the thermal behavior of the GaP nanoparticles under N_2 at different heating rates. A typical TGA profile is shown in Figure 5, and the results are completely in accord with the above conclusion.

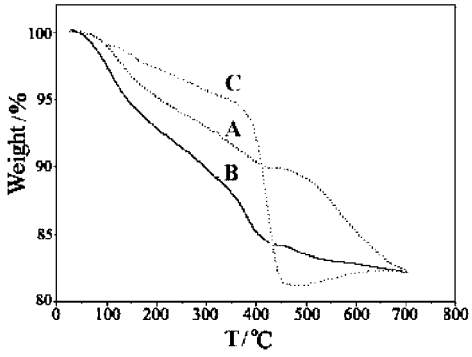

Figure 5. Thermogravimetric analyses of GaP nanocrystals in an N_2 flow at different heating rates; (A) 5 °C/min, (B) 10 °C/min, (C) 20 °C/min

One can see that at a heating rate of 5 °C/min [Figure 5 (A)], the weight loss is gradual, i.e. reaction (1) takes place during this process. The N and Ga atoms can be rendered miscible by an oxidation process since the N and Ga atoms can form a stable electrovalent bond, resulting in the final formation of GaN nanoparticles. At a heating rate of 10 °C/min, the weight loss is quicker than with a heating rate of 5 °C/min [Figure 5 (B)]. A precipitate line is obtained at a heating rate of 20 °C/min [Figure 5 (C)], indicating that the weight loss is much quicker than at the heating rates of 5 °C/min and 10 °C/min, namely, that reaction (2) takes place first followed by reaction (3) so the weight increases again later. The thermal stability results of GaP nanocrystalline under N_2 at different heating rates support the proposed mechanism that cubic GaN can form in GaP via a N−P metathesis mechanism.

Conclusion

In conclusion, a convenient, low-temperature technique has been established for the synthesis of cubic GaN nano-

crystals based on the fact that the small size effect of the starting GaP can remarkably reduce the difficulty of nitridation. Cubic GaN nanoparticles and nanorods have been successfully synthesized from the nitridation of nanocrystalline GaP at 500 °C for 30 min using a range of different heating rates. The thermal stability results of GaP nanocrystalline under N_2 at different heating rates support the proposal that cubic GaN can form in GaP via a N−P metathesis mechanism.

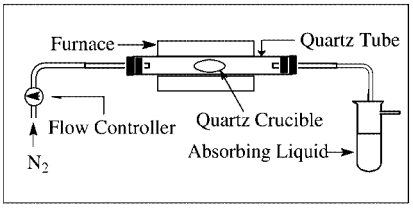

Figure 6. Schematic experimental setup for the formation of cubic GaN nanocrystals; GaP nanocrystals were placed in the quartz crucible

Experimental Section

Synthesis of Cubic GaN Nanocrystals: The starting GaP nanocrystals used in the present study were synthesized in the benzene-thermal route using Na_3P and $GaCl_3$ as the raw materials which has been described in detail elsewhere.[26] In a typical experiment, the starting GaP nanocrystals were loaded into a quartz crucible which was then horizontally placed in the quartz tube of a tubular furnace. The experimental setup for the formation of cubic GaN nanocrystals is described schematically in Figure 6. Firstly, the quartz tube was evacuated for 20 min. After this, the quartz tube was ventilated with high purity (99.999%) N_2 at a flow of about 20 sccm (standard cubic centimeters per minute) for several minutes, a unit mass flow controller was used to regulate the flow velocity of N_2 gas. The system was heated to 500 °C using different heating rates and then maintained at this temperature for 30 min. The samples were then allowed to cool to room temperature and were subsequently sealed in glass tubes for further characterization.

Characterization: Powder X-ray diffraction (XRD) patterns were obtained at room temperature using a Rigaku D/max-γA model X-ray diffractometer with Ni-filtered Cu-K_α radiation. TEM images of the samples were obtained from a Hitachi H800 transmission electron microscope using an accelerating voltage of 200 kV. Samples for TEM investigations were briefly ultra-sonicated in ethanol, and then a drop of suspension was placed on a holey copper grid with carbon film. X-ray photoelectron spectra (XPS) were measured on a VGESCALAB 220i-XL X-ray photo spectrometer with Al-K_α (1186.6 eV) radiation as the exciting source with measurements performed at pressures lower than 1×10^{-8} Torr. Thermogravimetric analyses (TGA) were performed on a Perkin−Elmer DC/2C type TG-DTA apparatus under a N_2 atmosphere at different heating rates. Fourier transform infrared spectra (FT-IR) of pellets of the samples mixed with KBr were recorded on a Nicolet Magna-IR 750 FTIR spectrometer at a resolution of 4 cm^{-1}.

Acknowledgments

We gratefully acknowledge financial support from the National Natural Research Foundation of China. We thank Dr. Y. W. Ding for his discuss of the TGA results.

[1] Y. Cui, C. M. Lieber, *Science* **2001**, *291*, 851.
[2] S. Sharma, M. K. Sunkara, *J. Am. Chem. Soc.* **2002**, *124*, 12288.
[3] X. F. Duan, Y. Huang, Y. Cui, J. F. Wang, C. M. Lieber, *Nature* **2001**, *409*, 66.
[4] S. J. Pearton, F. Ren, *Adv. Mater.* **2000**, *12*, 1571.
[5] G. P. Mitchell, C. A. Mirkin, R. L. Letsinger, *J. Am. Chem. Soc.* **1999**, *121*, 8122.
[6] D. L. Klein, R. Richard, A. K. L. Lin, A. P. Alivisatos, P. L. McEuen, *Nature* **1997**, *389*, 699.
[7] T. Somery, R. Werner, A. Forchel, M. Catalano, R. Cingolani, Y. Arakawa, *Science* **1999**, *285*, 1095.
[8] A. Argoitia, C. C. Hayman, J. C. Angus, L. Wang, J. S. Dyck, K. Kash, *Appl. Phys. Lett.* **1997**, *70*, 179.
[9] G. L. Wood, E. A. Pruss, R. T. Paine, *Chem. Mater.* **2001**, *13*, 12.
[10] J. A. Jegier, S. McKernan, A. P. Purdy, W. L. Gladfelter, *Chem. Mater.* **2000**, *12*, 1003 and references cited therein.
[11] J. L. Coffer, M. A. Johnson, B. L. Zhang, *Chem. Mater.* **1997**, *9*, 2671.
[12] A. Manz, A. Birkner, M. Kolbe, R. A. Fischer, *Adv. Mater.* **2000**, *12*, 569.
[13] D. Wang, S. Yoshida, M. Ichikawa, *Appl. Phys. Lett.* **2002**, *80*, 2472.
[14] D. Schikora, M. Hankeln, D. J. As, K. Lischka, T. Litz, A. Waag, T. Buhrow, F. Henneberger, *Phys. Rev. B* **1996**, *54*, R8381.
[15] T. Suski, H. Teisseyre, S. P. Lepkowski, P. Perlin, T. Kitamura, Y. Ishida, H. Okumura, S. F. Chichibu, *Appl. Phys. Lett.* **2002**, *81*, 232.
[16] A. P. Purdy, *Chem. Mater.* **1999**, *11*, 1648.
[17] W. Y. Wang, Y. P. Xu, D. F. Zhang, X. L. Chen, *Mater. Res. Bull.* **2001**, *36*, 2155.
[18] J. T. Hu, T. W. Odom, C. M. Lieber, *Acc. Chem. Res.* **1999**, *32*, 435.
[19] M. P. Azch, K. H. Ng, R. M. Penner, *Science* **2000**, *290*, 2120.
[20] Z. R. Dai, Z. W. Pan, Z. L. Wang, *J. Phys. Chem. B* **2002**, *106*, 902.
[21] W. S. Shi, Y. F. Zheng, N. Wang, C.-S. Lee, S.-T. Lee, *Adv. Mater.* **2001**, *13*, 591.
[22] X. Duan, J. Wang, C. M. Lieber, *Appl. Phys. Lett.* **2000**, *76*, 1116.
[23] X. Duan, C. M. Lieber, *Adv. Mater.* **2000**, *12*, 298.
[24] M. S. Gudiksen, C. M. Lieber, *J. Am. Chem. Soc.* **2000**, *122*, 8801.
[25] L. Grocholl, J. J. Wang, E. G. Gillan, *Chem. Mater.* **2001**, *13*, 4290.
[26] S. M. Gao, Y. Xie, J. Lu, G. A. Du, W. He, D. L. Cui, B. B. Huang, M. H. Jiang, *Inorg. Chem.* **2002**, *41*, 1850.
[27] S. M. Gao, J. Lu, Y. Zhao, N. Chen, Y. Xie, *Chem. Commun.* **2002**, 2880.
[28] S. M. Gao, J. Lu, N. Chen, Y. Zhao, Y. Xie, *Chem. Commun.* **2002**, 3064.
[29] S. M. Gao, J. Lu, Y. Zhao, N. Chen, Y. Xie, *Eur. J. Inorg. Chem.* **2003**, 1822.
[30] H. Yamane, M. Shimada, F. J. Disalvo, *Mater. Lett.* **2000**, *42*, 66.
[31] H. Yamane, T. Kajiwara, T. Sekiguchi, M. Shimada, *Jpn. J. Appl. Phys.* **2000**, *39*, L146.
[32] X. F. Duan, C. M. Lieber, *J. Am. Chem. Soc.* **2001**, *122*, 188.
[33] C. C. Chen, C. C. Yeh, *Adv. Mater.* **2000**, *12*, 738.
[34] J. A. Haber, P. C. Gibbons, W. E. Buhro, *J. Am. Chem. Soc.* **1997**, *119*, 5455.

Received June 2, 2003
Early View Article
Published Online December 4, 2003

